Magnetic Structure of $LaCrO_3$ Perovskite under High Pressure from *In Situ* Neutron Diffraction

J.-S. Zhou,[1] J. A. Alonso,[2] A. Muoñz,[3] M. T. Fernández-Díaz,[4] and J. B. Goodenough[1]

[1]*Texas Materials Institute, University of Texas at Austin, Austin, Texas 78712, USA*

[2]*Instituto de Ciencia de Materiales de Madrid, CSIC, Cantoblanco, E-28049 Madrid, Spain*

[3]*Departamento Física Aplicada, EPS, Universidad Carlos III, Avenida de la Universidad, 30, Leganés-Madrid, E-28911, Spain*

[4]*Institute Laue-Langevin (ILL) 156X, F-38042 Grenoble Cedex 9, France*

(Received 6 October 2010; published 31 January 2011)

The temperature-pressure phase diagram for both the crystal and magnetic structures of $LaCrO_3$ perovskite has been mapped out by *in situ* neutron-diffraction experiments under pressure. The system offers the opportunity to study the evolution of magnetic order, spin direction, and magnetic moment on crossing the orthorhombic-rhombohedral phase boundary. Moreover, a microscopic model of the superexchange interaction has been developed on the basis of the crystal structure obtained in this work to account for the behavior of T_N under high pressure.

DOI: 10.1103/PhysRevLett.106.057201 PACS numbers: 75.30.Kz, 75.25.−j, 75.30.Et

Antiferromagnetic ordering lowers the overall symmetry in a magnet. In most cases, magnetic structures can be described by irreducible representations of the symmetry of the crystal-structure [1]. Transition-metal oxides with the perovskite structure offer a variety of antiferromagnetic and ferromagnetic spin arrangements on the basis of the 23 tilting systems developed in the structure [2–4]. For the tilting system $a^+b^-b^-$ of the Glazer notation and the *Pbnm* space group, the relationship between magnetic structure and crystal structure has been illustrated by Bertaut in the 1960s [5]; he defined the *A*, *G*, *C*, and *F* magnetic modes according to the observed magnetic coupling between the 4 magnetic atoms present in the orthorhombic *Pbnm* unit cell. Among them, the *G* type stands for an isotropic antiferromagnetic coupling of a given atom with the six magnetic neighbors. In the presence of an anisotropic exchange interaction or the single-ion anisotropy, a canted-spin structure is developed. All possible canted-spin structures can also be specified in connection with the spin direction by irreducible representations. A huge number of studies in the literature have been focused on the structure with the *Pbnm* space group and its subgroup $P2_1/m$ since the space groups accommodate all antiferromagnetic and ferromagnetic spin-ordering phases [6]. Whereas both antiferromagnetic type-*G* and ferromagnetic phases have been found in mixed-valent perovskites with the $a^-a^-a^-$ tilting system of the *R*-3*c* space group [7,8], it has not been shown whether a single-valent rhombohedral perovskite can also accommodate type-*G* magnetic ordering.

The *R*-3*c* space group allows cooperative octahedral-site rotations about the [111] direction of the primary cubic unit cell or the *c* axis in the hexagonal setting. A few perovskite oxides $A^{3+}B^{3+}O_3$ with the geometric tolerance factor $t \equiv (A\text{-O})/[\sqrt{2}(B\text{-O})] \leq 1$ adopt the *R*-3*c* crystal structure at ambient pressure, e.g., $RAlO_3$ (R = La, Pr, Nd), $LaCoO_3$, $LaNiO_3$, $LaCuO_3$, $LaGaO_3$ (at $T > 540$ K). However, all these oxides are nonmagnetic. The rhombohedral (*R*) phase can also be stabilized under pressure, which increases the possibility to convert some magnetic perovskites with orthorhombic (*O*) structure into the *R* phase. The crystal structure of $LaMnO_3$ under 12 GPa has been refined well with the *R*-3*c* symmetry from x-ray diffraction data [9]. Unfortunately, the type-*A* antiferromagnetic phase collapses at the phase boundary because the structure of the *R* phase is not compatible with the Jahn-Teller (JT) distortion; an orbital ordering is required for the magnetic coupling in this JT-active system. The O/R phase transition in $LaFeO_3$ occurs at 1200 K [10], which is much higher than the Néel temperature $T_N \approx 740$ K [10]. Although T_N increases under pressure, it never meets the O/R phase boundary since a spin-state transition is induced at higher pressure [11]. In the perovskite nickelate $PrNiO_3$, the first-order metal-insulator–magnetic transition is completely suppressed under pressure before the O/R phase transition takes place [12]. The *O* phase of $LaCrO_3$ with the type-*G* antiferromagnetic spin ordering below T_N is perhaps the only candidate for us to explore how the magnetic phase enters the *R* phase under high pressure. The pressure-induced O/R phase transition at $P \approx 5.0$ GPa has been revealed by synchrotron diffraction studies under high-pressure [13,14]. Since the O/R transition at $T_t \approx 540$ K [14] under ambient pressure can be continuously reduced to room temperature under 5 GPa whereas $T_N = 298$ K at ambient pressure is expected to increase under pressure in this localized spin system, T_N may cross T_t at $P \geq 5$ GPa. Therefore, a magnetic structure study with neutron diffraction under pressure can reveal whether the type-*G* spin ordering collapses at T_t.

Neutron powder diffraction (NPD) experiments under pressure were performed at the high-flux D20 diffractometer with a Paris-Edinburgh device [15] in the Institut Laue-Langevin, France. Detailed information about NPD can be found in the supplemental materials (SM) [16].

A pressure scan at room temperature was first performed; NPD patterns were collected at pressure points 0.06, 0.70, 2.18, 4.00, 5.49, 5.79, 5.97, and 6.59 GPa. Figure 1 illustrates the quality of the NPD patterns of the O phase ($P = 2.18$ GPa) and the R phase ($P = 5.97$ GPa). Figure 2(a) shows the pressure dependences of lattice parameters at room temperature. The O/R phase transition occurs at $P_c \approx 5$ GPa where we have observed the two-phase coexistence; at $P = 5.5$ GPa, the refinement shows 90(1)% R phase in the sample. Results of the refinement from NPD data for both O and R structures under high pressure at room temperature can be found in Tables S1 and S2 in SM [16]. The *Pbnm* space group requires $b > a$ for rigid octahedra. However, the local site distortion, characterized by the O_{22}-Cr-O_{21} bond angle $\alpha \leq 90°$ that sets in from $GdCrO_3$ as the rare earth R^{3+} ionic radius increases in the $RCrO_3$ family [17,18], reduces lattice parameter b and eventually makes $b < a$ for $LaCrO_3$. High pressure appears to continuously increase a–b by further enlarging the local distortion.

The first-order transition to the R-3c phase occurs because the cubic phase cannot be achieved by continuously reducing the octahedral-site rotations in the O phase [17]. Moreover, the *Pbnm* space group is not a subgroup of the R-3c space group. A phase transition between these two space groups cannot be driven by continuously changing the tilting components. Since both structures consist of corner-shared octahedra, we are able to track down the changes of lattice parameters on crossing the phase transition through the relationship between these two unit cells. The most obvious change in the lattice parameters on passing P_c is along the c axis of the *Pbnm* cell. Fitting the V versus P curve with a third-order Birch-Murnagham equation of state gives a bulk modulus $B = 188 \pm 2$ GPa ($B' = 4$ fixed) for the O phase. We can also determine pressure-induced changes of atomic positions from the refinements. Figure 2(b) shows that the averaged Cr-O bond length shrinks almost continuously whereas a small jump of the Cr-O-Cr bond angle can be clearly seen on passing P_c as pressure increases.

Peaks of magnetic origin can be discerned at room temperature for $P \geq 2.2$ GPa, indicative of a $T_N > 300$ K. The inset of Fig. 1 highlights the main magnetic reflection in O and R phases. The magnetic structure of the O phase $LaCrO_3$ developed at ambient pressure has been refined in the G_x mode [6]. As for the R phase, the fit for the G_z structure is excellent. The results of refinements with all three possible magnetic structures can be found in SM [16]. In order to follow the thermal evolution of crystal and magnetic structures and to map out T_t in the T-P phase diagram, we collected neutron diffraction data while cooling down the sample at $P = 2.2$, 5.5, and 6.6 GPa. A first-order transition to reenter the O phase occurs at $T_t = 262$ K under 5.5 GPa. Figure S2 in SM [16] illustrates a characteristic range of the NPD patterns where the progression of the R/O transition is clearly followed upon cooling across the R/O boundary at 5.5 GPa. The same phase transition was observed at even lower temperature, $T_t = 175$ K under 6.6 GPa. A linear decrease of T_t versus P with a $dT_t/dP = -48.2 \pm 0.9$ K can be obtained in Fig. 2(c) from these data and T_t at ambient pressure from the literature [14].

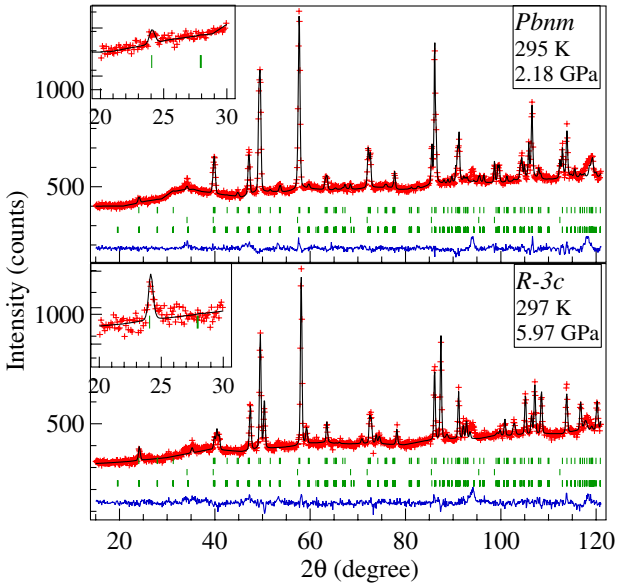

FIG. 1 (color online). Observed (crosses), calculated (full line), and difference NPD profiles for $LaCrO_3$ collected at 2.18 GPa and 5.97 GPa at room temperature. The three sets of Bragg reflections correspond to the main crystallographic phase, NaCl, and the magnetic phase. The insets show the main magnetic reflection. Small peaks near $2\theta = 94°$ and 118° come from the TiZr gasket.

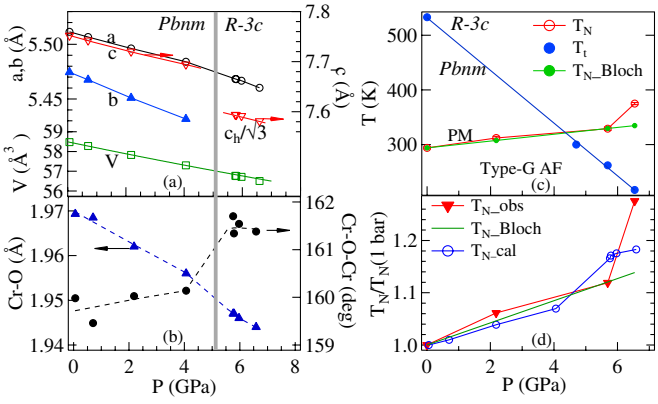

FIG. 2 (color online). (a),(b) Pressure dependences of lattice parameters and the average Cr-O bond length and Cr-O-Cr bond angle of $LaCrO_3$ at room temperature. Dashed lines inside the figure are a guide to the eyes. (c) The temperature-pressure phase diagram and (b) the pressure dependence of the normalized T_N and T_N calculated by a microscopic model and the Bloch rule for $LaCrO_3$.

Figure 3 shows the temperature dependence of the ordered magnetic moment $M(T)$ at Cr^{3+} under three pressures. Fitting these data with the Brillouin function gives T_N and the magnetic moment M_0 at 0 K. The R/O phase transition causes a discontinuous change at T_t, which can be seen clearly in the curve of $M(T)$ under $P = 5.5$ GPa. The curve fitting at $P = 5.5$ GPa was made to data points within the R phase shown in the inset of Fig. 3. Data points in the O phase point to a slightly lower T_N than that in the R phase at $P = 5.5$ GPa. It is important to know that the curve fittings to the data of both the O phase under $P = 2.17$ GPa and the R phase under $P = 5.5$ GPa give an $M_0 = 3.0\ \mu_B/\mathrm{Cr}$, which indicates that a localized-electron model remains applicable in the O and R phases. Although T_N increases progressively under pressure, M_0 for the $M(T)$ curve under $P = 6.6$ GPa is clearly lower than those at lower pressures. As mapped in Fig. 2(c), T_N increases with pressure nearly linearly to $P = 5.6$ GPa and does not show a jump at the O/R phase boundary. T_N at 6.6 GPa clearly deviates from the line of T_N versus P obtained at lower pressures. The *in situ* neutron-diffraction data under pressure also provide information for us to study the change of spin structure on crossing the O/R phase boundary and to test whether the superexchange formula can account for the pressure dependence of T_N on the basis of crystal-structure changes.

The superexchange interaction theory gives a relationship between the magnetic-coupling parameter J and the orbital overlap integral b by $J \propto b^2/U$, where U is the *on site* Coulomb energy. The Néel temperature can be calculated through a mean-field formula $k_B T_N = 4S(S+1)J$, S is the total spin on a magnetic ion. By using the formula of exchange coupling $J(\mathrm{Cr\text{-}O, Cr\text{-}O\text{-}Cr})$ in SM [16] and the structural data in Fig. 2, we can calculate the pressure dependence of the normalized T_N as a function of pressure

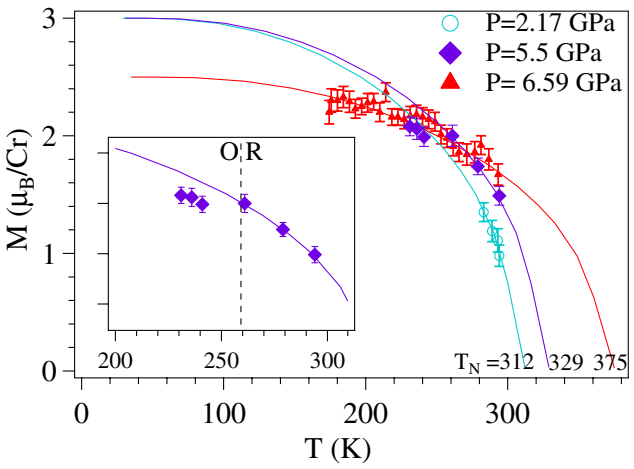

FIG. 3 (color online). Temperature dependence of magnetic moment M at Cr^{3+} under three different pressures; the inset shows the blowup plot of $M(T)$ under $P = 5.5$ GPa. Solid lines inside the figure are curve fittings to the Brillouin function.

in Fig. 2(d). This microscopic model works reasonably well to catch the essential feature of $T_N(P)$ observed.

Bloch [19] put forward a phenomenological rule on the basis of experimental results of antiferromagnetic transition-metal oxides, $\alpha \equiv (d \ln T_N/dP)/\kappa \approx 3.3$, where the compressibility κ can be calculated from the equation of state. Based on the $\kappa = B^{-1}$ from this work, we have calculated the $T_{N_{\mathrm{Bloch}}}$ in Fig. 2(c). The prediction based on the Bloch rule fits the $T_N(P)$ data well for $P \leq 6$ GPa. In the perovskite structure, the orbital overlap integral b is related to the bond length and the bond angle, not directly related to the cell volume. It remains open why the Bloch rule based on the volume change can account for the pressure dependence of T_N in the perovskite $LaCrO_3$.

Although the microscopic model and the Bloch rule work successfully at low pressures, neither can account for a dramatic T_N jump at 6.6 GPa. A significant deviation from the Bloch rule has been observed in systems such as $LaMnO_3$ [20] and $SmNiO_3$ [21]. Deviation from the Bloch rule can be caused either by the breakdown of the perturbation expression of the superexchange interaction or by a volume change that is no longer correlated to the change of the orbital overlap integral. In the case of perovskite $LaCrO_3$, failure of the microscopic model suggests that the localized electronic state is at the brink of collapse under 6.6 GPa. Corresponding to a T_N jump, the M_0 of $LaCrO_3$ under 6.6 GPa shows a noticeable reduction, which is consistent with a collapsing of the localized electronic state at Cr^{3+}. This argument deserves to be verified by other experimental probes under high pressure.

The orthorhombic $LaCrO_3$ perovskite exhibits the type-G antiferromagnetic spin order at ambient pressure, which is consistent with the superexchange rules for t^3-O-t^3 coupling. However, the spin-ordering direction is degenerate. The group theory set by Bertaut gives two possible configurations for type-G spin order in the *Pbnm* space group, i.e., (F_x, C_y, G_z) or (G_x, A_y, F_z). Magnetic susceptibility $\chi(T)$ is the most sensitive probe to detect spin canting. Instead of a cusp, an abrupt increase of $\chi(T)$ at T_N in Fig. 4 is characteristic of canted-spin ordering. However, neither the anomaly of $\chi(T)$ nor the refinements of the magnetic structure from NPD data under pressure in the orthorhombic phase could distinguish these two modes. We have chosen the solution (G_x, A_y, F_z) since the mode (F_x, C_y, G_z) occurs only in the case where the rare-earth ion R is magnetic or the octahedral site is highly distorted. Spins in the (G_x, A_y, F_z) mode are pointed to the octahedral edge in the O_{22}-Cr-O_{21} plane as illustrated in Fig. 4. The spin canting direction allowed by the symmetry follows the cooperative octahedral-site rotation, which gives the ferromagnetic component along the c axis. The spin reorientation on crossing the O/R phase transition in $LaCrO_3$ under high pressure provides a nice example of the relationship between the crystal symmetry and magnetic structure. Although the localized electron model describing the

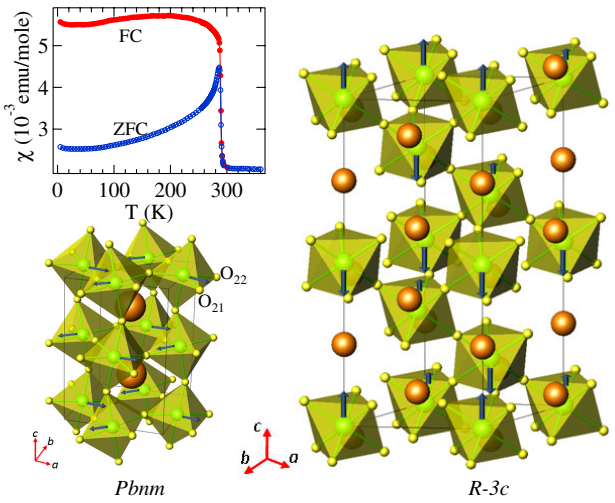

FIG. 4 (color online). Crystal structures of *Pbnm* and *R*-3*c* phases with corresponding spin ordering at Cr^{3+} ions. Inset: temperature dependence of the magnetic susceptibility of $LaCrO_3$. The magnitude of spin canting in the *Pbnm* phase is exaggerated for clarification.

exchange interaction through the t^3-O-t^3 in the perovskite $LaCrO_3$ remains valid on crossing the phase transition, the *R*-3*c* group symmetry only allows the antiferromagnetic spin structure with the spin direction along the *c* axis, i.e., the axis of highest rotation symmetry in this space group. Therefore, on crossing the O/R phase boundary, the spin direction in the type-*G* antiferromagnetic phase rotates from pointing to the octahedral edge to perpendicular to the triangle plane of an octahedron in Fig. 4.

In conclusion, the first-order orthorhombic to rhombohedral phase transition T_t in perovskite $LaCrO_3$ decreases linearly as pressure increases with a slope $dT_t/dP = -48.2$ K/GPa. On crossing the O/R phase transition, the symmetry change of the crystal structure does not alter the localized-electron regime and type-*G* antiferromagnetism, but it causes a spin reorientation from a spin direction pointing to the edge to one pointing to the triangular face of an octahedron. The possibility of canting the spin structure of the *Pbnm* phase is eliminated in the *R*3-*c* phase. This study has revealed a rule for spin direction in antiferromagnetic perovskites RMO_3: (1) it is parallel to the rotation axis with the highest symmetry in the space group; (2) if there are more than one rotation axis in the space group, it is determined by either higher-order orbital angular momentum or the *R*-*M* exchange interaction for the magnetic rare earth. The behavior of the antiferromagnetic transition temperature T_N under high pressure in both the *O* and *R* phases can be quantitatively accounted for either by a microscopic superexchange model based on the crystal structure obtained from this study or by a phenomenological Bloch rule for $P < 6$ GPa. A dramatic increase of T_N accompanied by a clear reduction of magnetic moment in the *R* phase under $P \geq 6.5$ GPa signals a breakdown of the localized-electron picture in $LaCrO_3$.

This work was supported by NSF (DMR 0904282) and the Robert A. Welch Foundation (Grant No. F-1066), as well as the Spanish Ministry of Science and Innovation (MAT2010-16404).

*jszhou@mail.utexas.edu

[1] Yu A. Izyumov, Sov. Phys. Usp. **23**, 356 (1980).
[2] R. H. Mitchell, *Perovskites, Modern and Ancient* (Almaz Press, Ontario, 2002).
[3] E. O. Wollan and W. C. Koehler, Phys. Rev. **100**, 545 (1955).
[4] J. Rodriguez-Carvajal *et al.*, Phys. Rev. B **57**, 456 (1998).
[5] E. F. Bertaut, in *Magnetism*, edited by G. T. Rado and H. Suhl (Academic Press, New York, 1963), Vol. III, p. 149.
[6] J. B. Goodenough and J. M. Longo, in *Crystallographic and Magnetic Properties of Perovskite and Perovskite-related Compounds*, edited by K.-H. Hellwege, Landolt-Bornstein, New Series, Group III, Vol. 4a (Springer-Verlag, Berlin, 1970), p. 126.
[7] K. Tezuka *et al.*, J. Solid State Chem. **141**, 404 (1998).
[8] A. Urushibara *et al.*, Phys. Rev. B **51**, 14 103 (1995).
[9] J.-S. Zhou *et al.*, Phys. Rev. B **78**, 220402(R) (2008).
[10] R. Dogra *et al.*, Phys. Rev. B **63**, 224104 (2001).
[11] W. M. Xu *et al.*, Phys. Rev. B **64**, 094411 (2001).
[12] J.-S. Zhou, J. B. Goodenough, and B. Dabrowski, Phys. Rev. Lett. **94**, 226602 (2005).
[13] T. Hashimoto *et al.*, Solid State Commun. **108**, 691 (1998).
[14] T. Shibasaki *et al.*, J. Therm. Anal. Calorim. **81**, 575 (2005).
[15] S. Klotz *et al.*, High Press. Res. **14**, 249 (1996).
[16] See supplemental material at http://link.aps.org/supplemental/10.1103/PhysRevLett.106.057201 for detailed information on refinements from neutron diffraction and the formula of superexchange interaction in $RCrO_3$.
[17] J.-S. Zhou and J. B. Goodenough, Phys. Rev. Lett. **94**, 065501 (2005).
[18] J.-S. Zhou *et al.*, Phys. Rev. B **81**, 214115 (2010).
[19] D. Bloch, J. Phys. Chem. Solids **27**, 881 (1966).
[20] J.-S. Zhou and J. B. Goodenough, Phys. Rev. Lett. **89**, 087201 (2002).
[21] J.-S. Zhou, J. B. Goodenough, and B. Dabrowski, Phys. Rev. Lett. **95**, 127204 (2005).